J Polym Res (2017) 24: 47
DOI 10.1007/s10965-017-1204-9

ORIGINAL PAPER

Influence of molecular weight on scaling exponents and critical concentrations of one soluble 6FDA-TFDB polyimide in solution

Ensong Zhang[1,2] · Hongxiang Chen[1,2] · Xuemin Dai[2,3] · Xue Liu[1] · Wenke Yang[1,2] · Wei Liu[1,2] · Zhixin Dong[3] · Xuepeng Qiu[3] · Xiangling Ji[1]

Received: 3 November 2016 / Accepted: 13 February 2017 / Published online: 8 March 2017

Abstract Polyimde (PI) samples with different molecular weights were synthesized. Based on SEC coupled with multidetectors measurement and Yamakawa-Fujii-Yoshizaki (YFY) model, eight soluble samples with absolute M_w from 40,600 g/mol to 197,000 g/mol are chosen and applied to investigate the influence of molecular weight on scaling exponents and critical concentrations at 20–45 °C in dilute, semidilute unentangled, and semidilute entangled solutions. Most of the scaling exponents are higher than the theoretical values in three concentration regions, and scaling exponent increases with molecular weight; overlap concentration (C*) increases and entanglement concentration (C_e) decreases with molecular weight. Considering bead-bead interaction, corrected bead-spring model can explain the related results. Finally, the relationship among C^*, C_e, and molecular weight is established at different temperatures (from 20 °C to 45 °C), and two linear equations are available at each temperature. Thus, both C^* and C_e are calculated at a fixed molecular weight. And from C/C^* and C/C_e ratios, the morphology of PI fiber during electrospinning can be controlled. These results are helpful to guide the preparation of polyimide solutions for different processing.

Keywords Soluble polyimide · Scaling exponent · Critical concentration · Molecular weight

Electronic supplementary material The online version of this article (doi:10.1007/s10965-017-1204-9) contains supplementary material, which is available to authorized users.

✉ Xuepeng Qiu
xp_q@ciac.ac.cn

✉ Xiangling Ji
xlji@ciac.ac.cn

[1] State Key Laboratory of Polymer Physics and Chemistry, Changchun Institute of Applied Chemistry, Chinese Academy of Sciences, Changchun 130022, People's Republic of China

[2] University of Chinese Academy of Sciences, Beijing 100049, People's Republic of China

[3] Laboratory of Polymer Composites and Engineering, Changchun Institute of Applied Chemistry, Chinese Academy of Sciences, Changchun 130022, People's Republic of China

Introduction

In recent years, polyimide has become more and more important in various industrial products, such as resin, film, fiber, and foam [1–8]. However, conventional polyimide products such, as Kapton and Upilex, are insoluble in organic solvents, thereby inhibiting its applications in many fields. People found that introducing fluoroalkyl groups can inhibit π–π stacking and increase polarity, thereby facilitating solvent interaction with PI segments and increasing solubility [9].

Based on the scaling relationship between specific viscosity η_{sp} and concentration, the polymer solution can be divided into three different concentration regions: dilute (below overlap concentration C^*, polymer chains act as coils and separate apart from each other in solution); semidilute unentangled (when $C^* < C < C_e$, polymer coils overlap with each other and dominate the physical properties of solution) and semidilute entangled (when polymer concentration above entanglement concentration C_e, polymer chains begin to entangle with each other and influence the dynamic properties of solution). Thus, on the basis of different concentration, it is necessary to discuss the properties of polymer solution separately.

In our previous work [10], one soluble PI was synthesized by polycondenzation of 2,2′-bis(trifluoromethyl)-4,4′-diaminobiphenyl (TFDB) and 2,2-bis(3,4-dicarboxy- phenyl) hexafluoropropane dianhydride (6FDA), and it exhibited good solubility in DMF and THF in various concentration ranges.

Scheme 1 Synthetic procedure of 6FDA-TFDB polyimide sample

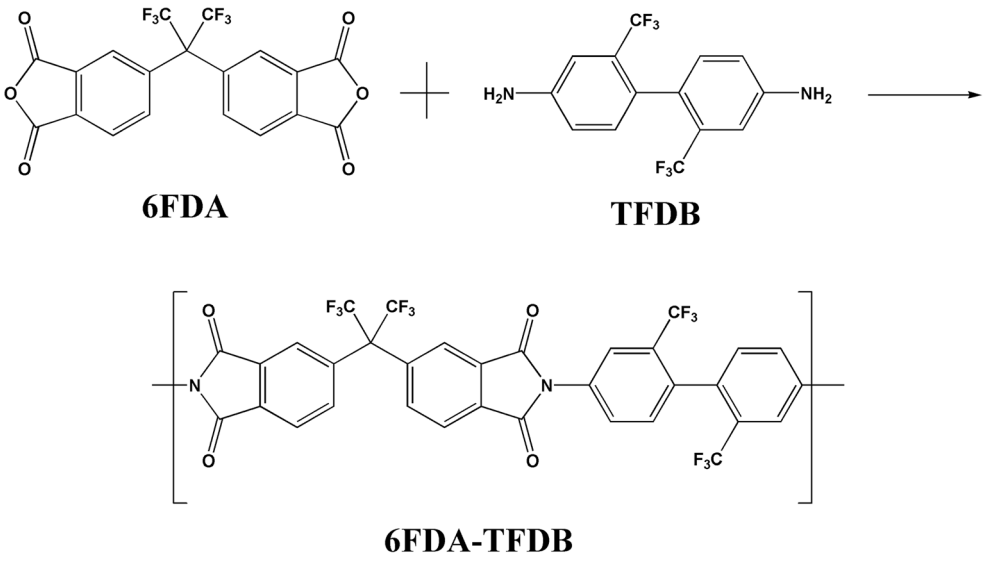

Based on rheological data and scaling theory, scaling relationship between specific viscosity (η_{sp}) and concentration is established, and influence of factors on critical concentration and scaling exponents are discussed [10]. It is demonstrated that dipole-dipole interaction is the main factor for inducing the deviation of scaling exponents from dilute to semidilute entangled solution.

Definitely, molecular weight of polyimide is one of the most important factors in the process. Liu and coworkers studied two isomerized polyimides and found that soluble PI chain acts as a flexible chain with local rigidity [11, 12]. That is, if the molecular weight decreased to a critical value, polyimide chain behavior will become rigid. Moreover, for samples with low molecular weight, entanglement points are not enough among polyimide chains, which will influence final product application. Thus, it is necessary to analyze the solution behavior of polyimide samples with different molecular weights in different concentration ranges.

The relationship between scaling exponent and molecular weight for neutral polymer was studied in literature [13]. Pankaj et al. synthesized poly(methyl methacrylate) (PMMA) samples with different molecular weights (M_w from 12,470 g/mol to 365,700 g/mol) and studied the relationship between η_0 and concentration. However, for samples with different molecular weights, all data was in one straight line in the same concentration regime, i.e., scaling exponent is independent of molecular weight. However, as demonstrated in our previous work, the behavior of this polyimide solution cannot be described as neutral polymer solution. Thus, it is necessary to analyze the relationship between scaling exponent and molecular weight in different concentration ranges.

In this study, soluble 6FDA-TFDB polyimides with different molecular weights are synthesized and fractionated. Using size exclusion chromatography (SEC) coupled with multidetectors,

Table 1 Molecular weight information for 6FDA-TFDB PI samples

Sample	Absolute M_w	PDI	R_g (nm)
PI-1.4 W	14,600	1.31	8.1
PI-1.5 W	15,600	1.40	6.6
PI-2.7 W	27,300	1.50	6.7
PI-3.3 W	32,900	1.19	7.4
PI-4.1 W	40,600	1.38	9.0
PI-5.5 W	55,200	1.23	11.1
PI-5.6 W	56,200	1.18	11.4
PI-6.8 W	68,000	1.16	12.4
PI-7.9 W	79,400	1.25	14.5
PI-9.2 W	92,300	1.40	15.4
PI-10 W	104,000	1.27	17.0
PI-11 W	108,000	1.25	17.3
PI-12 W	116,000	1.45	18.4
PI-13 W	133,000	1.25	18.7
PI-14 W	136,000	1.22	19.1
PI-20 W	197,000	1.40	24.3

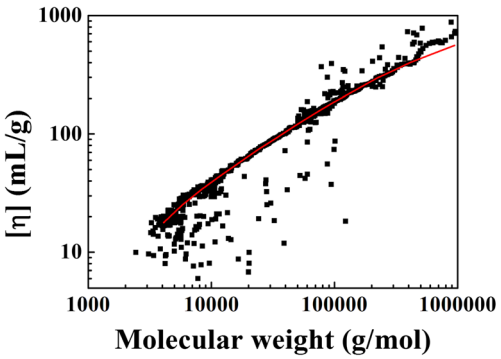

Fig. 1 Relationship between intrinsic viscosity and molecular weight from SEC coupled with viscometer detector. Data was fitted by PI-1.4 W, PI-4.1 W and PI-12 W three different molecular weight PI samples

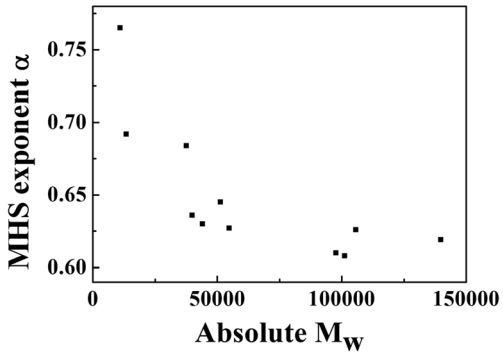

Fig. 2 Variation of the Mark-Houwink-Sakurada (MHS) exponent α with molecular weight for PI samples

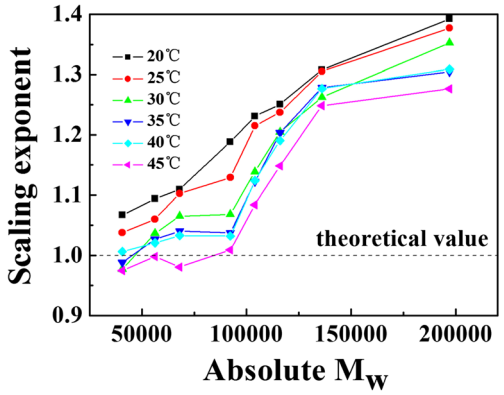

Fig. 3 Relationship between scaling exponent and molecular weight in dilute solution

the absolute weight-average molecular weight M_w, the radius of gyration R_g, the intrinsic viscosity [η] can be obtained and the relationship among them can be established. Based on YFY model, soluble polyimide samples with different molecular weights (absolute M_w from 40,600 g/mol to 197,000 g/mol) are chosen. Based on rheological data and scaling theory, the scaling relationship between specific viscosity (η_{sp}) and concentration is established, and the influence of molecular weight on critical concentration and scaling exponents are extensively discussed.

Experimental

Chemicals

2,2′-Bis(trifluoromethyl)-4,4′-diaminobiphenyl (TFDB), 2,2-bis(3,4-dicarboxy- phenyl)hexafluoro- propane dianhydride (6FDA) , were purchased from Beijing Multi Technology. Before reaction, all the materials were purified by sublimation. In order to reduce the effect of water, N,N-dimethylacetamide (DMAc) was dried in the presence of P_2O_5 overnight and the reaction was carried out at the room temperature with relative humidity less than 50%. N,N-dimethylformamide (DMF) as solvent was spectrum purification. Tetrabutylammonium bromide (TBAB, AR) was purchased from Sinopharm Chemical Reagent Co., Ltd. Other chemicals were used as received without further purification.

Table 2 l_p, M_L and d for PI sample in DMF with 3.1 mM TBAB at 35 °C

Sample	l_p[a] (nm)	M_L (nm^{-1})	d (nm)	l_p[b] (nm)
PI-4.1 W	2.22	212	0.519	2.18

[a] l_p is estimated from Eq. (3)–(8) with intrinsic viscosity and molecular weight

[b] l_p is estimated from Eq. (10) with z-average radius of gyration and molecular weight

Synthesis of polyamic acid (PAA) solution

In 3 L three-necked flask, 0.35 mol TFDB was added in approximately 1600 mL of N,N-dimethylacetamide (DMAc), stirred until TFDB was dissolved completely. Then the same molar amount of 6FDA and different amount of *o*-phthalic anhydride (end capping agent) were added and the mixture was stirred for 48 h at ambient temperature under nitrogen atmosphere.

Synthesis of polyimide (PI)

0.7 mol triethylamine and 1.4 mol acetic anhydride were added into the above PAA solution, the mixture reacted for 4 h to yield homogeneous solution. Then the solution was poured slowly into methanol for precipitation. The solid was washed thoroughly with methanol, and then redissolved in DMAc and precipitated in methanol again to obtain a purified sample. Finally, it was imidized and dried in a vacuum tube at 350 °C. The synthetic procedure for 6FDA-TFDB polyimide was shown in Scheme 1.

Precipitation fractionation of PI sample

PI sample (6FDA-TFDB) was dissolved in THF to get 1 wt% PI solution in 2000 mL round-bottomed flask, then the temperature was raised to 25 °C (5 °C higher than the room temperature) and kept at least 24 h to make sure a homogeneous solution. Then the water as a precipitator was added dropwise to above PI solution. When enough water was added in the solution, the precipitation appeared. Then appropriate amount of water was added to make the solution turbid enough, and the temperature was kept at 25 °C at least 24 h to reach an equilibrium of dissolution-precipitation. Then the precipitated PI sample was collected by centrifugation (8000 rpm, 20 min), washed by water twice and dried in vacuum. The filtrate was repeated the previous step several times to get different fractions.

Table 3 Scaling exponents of PI samples with different molecular weights at different temperatures in dilute solution

Sample	20 °C	25 °C	30 °C	35 °C	40 °C	45 °C
PI-4.1 W	1.07 ± 0.04	1.04 ± 0.04	0.98 ± 0.06	0.99 ± 0.05	1.01 ± 0.06	0.97 ± 0.06
PI-5.6 W	1.09 ± 0.04	1.06 ± 0.03	1.03 ± 0.02	1.03 ± 0.01	1.02 ± 0.01	1.00 ± 0.01
PI-6.8 W	1.11 ± 0.00	1.10 ± 0.04	1.06 ± 0.00	1.04 ± 0.02	1.03 ± 0.11	0.98 ± 0.12
PI-9.2 W	1.18 ± 0.03	1.13 ± 0.01	1.07 ± 0.01	1.04 ± 0.02	1.03 ± 0.02	1.01 ± 0.02
PI-10 W	1.19 ± 0.03	1.17 ± 0.02	1.14 ± 0.03	1.10 ± 0.01	1.12 ± 0.04	1.06 ± 0.05
PI-12 W	1.25 ± 0.02	1.23 ± 0.01	1.20 ± 0.01	1.20 ± 0.01	1.19 ± 0.01	1.14 ± 0.02
PI-14 W	1.31 ± 0.06	1.30 ± 0.05	1.26 ± 0.04	1.28 ± 0.04	1.28 ± 0.04	1.25 ± 0.03
PI-20 W	1.40 ± 0.04	1.38 ± 0.06	1.35 ± 0.05	1.30 ± 0.05	1.31 ± 0.07	1.28 ± 0.05

Measurements

FT-IR and ^{1}H NMR measurements

Fourier transform infrared (FTIR) spectra were recorded on a Brucker Vertex 70 spectrometer. ^{1}H NMR spectra were recorded using a Bruker AV400 NMR spectrometer in deuterated trichloromethane ($CDCl_3$ with 0.05% *v*/v TMS).

Size exclusion chromatography with multi-detectors tests

Size exclusion chromatography (SEC) coupled with multidetectors systems consists of a 515 pump (Waters Technologies), a 717 autosampler (Waters Technologies), two PL-gel 10 μm Mixed B-LS columns (Agilent Technologies), a DAWN HELEOS II multi-angle laser light scattering detector (MALLS) (Wyatt Technologies), a ViscoStar Viscometer (Wyatt Technologies) and a 2414 refractive index detector (RI) (Waters Technologies). The SEC system was operated at 35 °C using DMF with 3.1 mM TBAB as the mobile phase at a flow rate of 1 mL/min. In order to get the absolute molecular weight, the following procedure was carried out. (1) To get the optical constant of MALLS, the chromatographic toluene was used as mobile phase. And the optical constant can be calculated by ASTRA V5.3.4 software. (2) To get the refractive index increment (*dn/dc*) of different molecular weight PI samples, five different concentrations (from 1 mg/mL to 5 mg/mL) were injected and *dn/dc* value can be obtained from the slope of line. The results were listed in Table S1. (3) Correction of scattering volume of different angle was carried out using narrow distribution PS standard (nominated M_w 30,000). (4) Absolute weight-average molecular weight, radius of gyration and exponent α in Mark-Houwink-Sakurada (MHS) equation were determined using ASTRA V5.3.4 software (Wyatt Technologies).

Rheological tests

All rheological measurements for PI/DMF solutions were carried out with a TA instruments DHR-2 stress-controlled rheometer where a 40 mm, 2° cone plate geometry was used. Temperature-controlled Peliter plate was used to control the temperature. The sweep of frequency was chosen from 1 to 1000 rad/s. In order to prevent the evaporation of solvent, two semicircle iron plates with radius of 60 mm were covered around the plate geometry, and silicone grease was filled around the gap of the iron plates.

Basic characterization of PI samples

Figures S1 and S2 confirmed the chemical structure of PI samples. For FT-IR result, the peak at 1786 cm^{-1} was assigned to C = O asymmetric stretching vibration; the peak at 1726 cm^{-1} came from C = O symmetric stretching vibration;

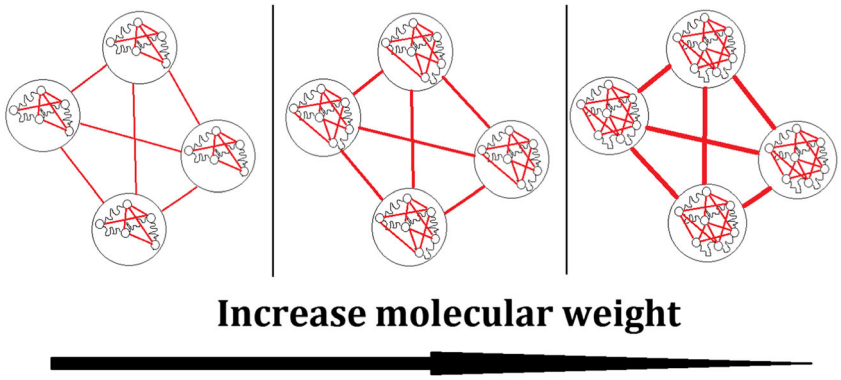

Fig. 4 Schematic of interaction of polymer coils with molecular weight

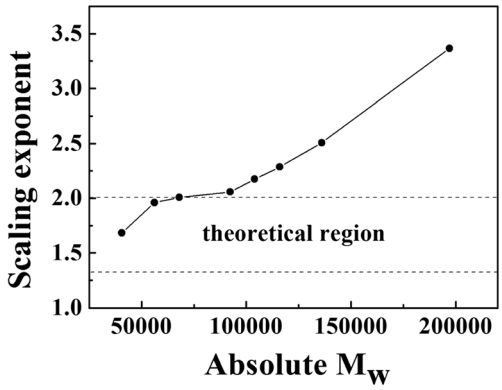

Fig. 5 Relationship between scaling exponent and molecular weight in semidilute unentangled solution at 20 °C

the peak at 1364 cm^{-1} was due to C-N stretching vibration. These three peaks indicated the presence of imide ring. For ^1H NMR result, the resonance signals from different positions are as follows: δ 8.22 (d, J = 7.6 Hz, 2H), δ 7.98 (s, 2H), δ 7.94 (m, 4H), δ 7.75 (d, J = 8.2 Hz, 2H), δ 7.52 (d, J = 8.2 Hz, 2H). Moreover, from the ^1H NMR result, we cannot detect the signal of –COOH and –NH- group, which demonstrated that the polyimide is fully imidized. Fig. S3 was GPC curves and detailed information on molecular weight of samples was listed in Table 1.

Results and discussion

Selection of samples

Based on Mark-Houwink-Sakurada (MHS) equation:

$$[\eta] = KM^{\alpha} \tag{1}$$

The exponent α can be obtained from the slope between [η] and M_w [14]. Using SEC-multidetector system, absolute M_w and the exponent α in Mark-Houwink-Sakurada (MHS) equation of PI samples can be obtained. Figure 1 is the relationship between [η] and molecular weight of PI sample in a wide molecular weight range. It can be seen that, the slope between [η] and M_w increases as the molecular weight decreases. And Fig. 2 shows that as the M_w is below 30,000 g/mol, the exponent α is in the range of 0.68 ~ 0.76 and decreases with M_w, which indicates that the PI chains become rigid in solution. When molecular weight is larger than 30,000, exponent α is in the range of 0.61 ~ 0.64, indicating flexible chains in good solvent.

As previous work reported [11, 12], soluble PI chain acts as a flexible chain with local rigidity. Thus, it is necessary to use Kratky-Porod wormlike chain model [15] to analyze the PI chain. Yamakawa-Fujii-Yoshizaki (YFY) proposed wormlike cylinder model [16], which can be used to evaluate the persistent length (l_p) of semi-flexible molecules. The relationship between [η] and molecular weight for unperturbed polymer chain can be expressed as [16–18]:

$$[\eta]_0 = \left[\Phi_{0,\infty}\left(\langle h^2\rangle_0/M\right)^{3/2}M^{1/2}\right]\Gamma_1(L,D,l_p) \tag{2}$$

where $\Phi_{0,\infty}$ is a constant, $\Phi_{0,\infty} = 2.87*10^{23}$; $<h^2>_0$ is mean square end-to-end distance; $\Gamma_1(L, d, l_p)$ is a function of contour length L, polymer chain diameter d and persistence length l_p. According to YFY theory, it is suitable to express the polymer chain behavior of (1) rodlike at low M, (2) wormlike at intermediate M, (3) random coil at high M.

Bohdanecky introduced an approximate expression for $\Gamma_1(L, d, l_p)$, which can be expressed as [18]:

$$\left(M^2/[\eta]_0\right)^{1/3} = A_\eta + B_\eta M^{1/2} \tag{3}$$

$$A_\eta = A_0 M_L \Phi_{0,\infty}^{-1/3} \tag{4}$$

$$B_\eta = B_0 \Phi_{0.\infty}^{-1/3}\left(2l_p/M_L\right)^{-1/2} \tag{5}$$

where M_L is the shift factor; B_0 is a constant, $B_0 = 1.05$; A_0 is a parameter related to the reduced backbone diameter d_r, $d_r = d/2l_p$. The result is shown in Fig. S4. Good linearity over a wide molecular weight range is obtained, which demonstrates that YFY theory can describe the PI chain behavior (the deviation at $M > 10^6$ results from the excluded volume effect [18]). A_η and B_η can be obtained from the intercept and slope, respectively.

Table 4 Scaling exponents of PI samples with different molecular weights at different temperatures in semidilute unentangled solution

Sample	20 °C	25 °C	30 °C	35 °C	40 °C	45 °C
PI-4.1 W	1.68 ± 0.05	1.65 ± 0.04	1.62 ± 0.04	1.62 ± 0.04	1.61 ± 0.03	1.60 ± 0.04
PI-5.6 W	1.96 ± 0.06	1.96 ± 0.05	1.95 ± 0.13	1.95 ± 0.06	1.94 ± 0.08	1.88 ± 0.08
PI-6.8 W	2.01 ± 0.10	2.01 ± 0.12	2.01 ± 0.11	2.02 ± 0.10	2.01 ± 0.09	2.01 ± 0.07
PI-9.2 W	2.06 ± 0.05	2.04 ± 0.06	2.03 ± 0.04	2.03 ± 0.04	2.03 ± 0.03	2.03 ± 0.03
PI-10 W	2.17 ± 0.13	2.17 ± 0.13	2.15 ± 0.13	2.12 ± 0.13	2.12 ± 0.12	2.10 ± 0.14
PI-12 W	2.29 ± 0.02	2.26 ± 0.03	2.24 ± 0.03	2.23 ± 0.03	2.23 ± 0.03	2.21 ± 0.02
PI-14 W	2.51 ± 0.04	2.50 ± 0.04	2.50 ± 0.04	2.50 ± 0.04	2.49 ± 0.04	2.49 ± 0.05
PI-20 W	3.37 ± 0.03	3.39 ± 0.03	3.41 ± 0.03	3.41 ± 0.04	3.46 ± 0.06	3.49 ± 0.09

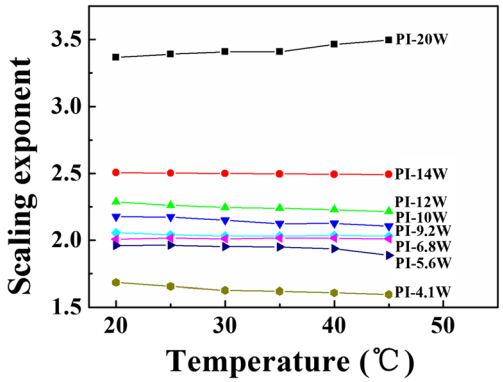

Fig. 6 Variation of scaling exponents of PI samples with molecular weights at different temperatures in semidilute unentangled solution

For A_0, it is related to reduced backbone diameter d_r

$$d_r^2/A_0 = 4\Phi_{0,\infty}B_\eta^4/\left(1.215\pi N_A \rho A_\eta\right) \quad (6)$$

$$\log\left(d_r^2/A_0\right) = 0.173 + 2.518\log d_r \quad (d_r \le 0.1) \quad (7)$$

$$\log\left(d_r^2/A_0\right) = 0.795 + 2.78\log d_r \quad (0.1 \le d_r \le 0.4) \quad (8)$$

where N_A is Avogadro's constant and ρ is the density of solute. The density of our sample is 1.38 g/cm^3. Thus, l_p, M_L and d can be calculated from the equation above, and the results are listed in Table 2. Compared with some flexible polymer chain results, the PI persistence length l_p (2.22 nm) is larger than polystyrene in cyclohexane (0.9 ~ 1.0 nm), PMMA in benzene (1.4 nm); but much smaller than trinitrocellulose in acetone (14.5 nm) [19].

The length of monomer l_u can be calculated from bond length and bond angle [20], l_u = 2.15 nm. It can be seen that, the local rigidity of PI chain comes from the rigidity of monomer. The contour length L can be calculated from the equation below:

$$L = nL_u = M_w/M_u l_u \quad (9)$$

From the light scattering result, for PI-4.1 W sample, the contour length L = 120.1 nm, and $L/l_p = 54.1 \gg 1$. And it can be regarded as a flexible chain.

Moreover, based on the radius of gyration, we can also calculate the persistence length from the equation below [21]

$$\left\langle R_g^2 \right\rangle_0 = l_p^2\left[2\left(\frac{L}{l_p} - 1 + \exp\left(-\frac{L}{l_p}\right)\right)\left(\frac{l_p}{L}\right)^2 - 1 + \frac{1}{3}\frac{L}{l_p}\right] \quad (10)$$

For PI-4.1 W, l_p = 2.18 nm, which is nearly the same as the result of YFY model.

Based on the above results, eight samples with higher molecular weights, PI-4.1 W, 5.6 W, 6.8 W, 9.2 W, 10 W, 12 W, 14 W, and 20 W, from 40,600 g/mol to 197,000 g/mol, are chosen for this study.

Relationship between scaling exponent and molecular weight of PI samples in dilute solution

The theory predicts that, based on the relationship between η_{sp} and concentration, the scaling exponent is 1.0 for neutral polymer in dilute solution [27]. And Fig. 3 shows the relationship between scaling exponent and molecular weight of PI samples at different temperatures in dilute solution. The details are also listed in Table 3. The black line shows the theoretical scaling exponent in dilute solution. From PI-4.1 W to PI-20 W at 20 °C, scaling exponent increases from 1.07 to 1.40; at 45 °C, corresponding scaling exponent increases from 0.97 to 1.28. Almost all the scaling exponents are higher than the theoretical value of 1.0, and they increase as the molecular weight increases and temperature decreases. The scaling exponents for PI-4.1 W at 30–45 °C are very close to 1.0.

In our previous work [10], scaling exponent deviation had been discussed, and it was found that polymer coils tend to interact with each other due to heterogeneity in dilute polymer solution. Here, corrected bead-spring models are applied to explain the above result. Increasing the molecular weight makes the number of beads and spring increase, which increases the interaction between beads (see Fig. 4). Moreover, increasing molecular weight makes dilute polymer solution

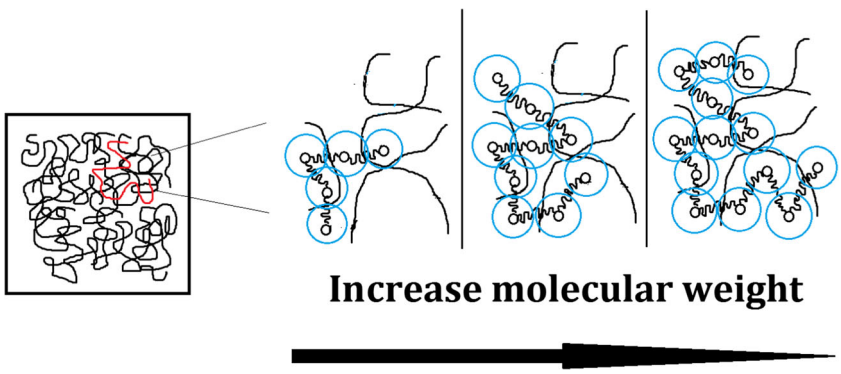

Fig. 7 Schematic of interchain interaction with molecular weight of PI samples in semidilute unentangled solution

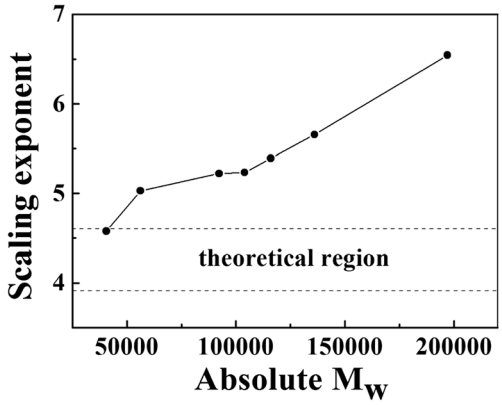

Fig. 8 Relationship between scaling exponent and molecular weight of PI samples at 20 °C in semidilute entangled solution

become more heterogeneous. Increasing the interaction between beads decreases polymer coil radius, which increases the heterogeneity of dilute polymer solution. The result of the relationship between overlap concentration and temperature also demonstrates this. Finally, interaction between polymer coils and deviation of scaling exponent both increase.

Raising the temperature can also increase Brownian motion of polymer coils, which weakens the interaction between polymer coils and decreases the deviation of scaling exponent. In fact, for PI-4.1 W, when temperature reaches a critical value (30 °C), scaling exponent decreases to theoretical region. That is, the interaction between polymer coils is too small to influence the scaling exponent. Above 30 °C, the interaction between polymer coils cannot influence the scaling exponent, and the scaling exponent remains at constant.

Relationship between scaling exponent and molecular weight of PI samples in semidilute unentangled solution

The theory predicts that, based on the relationship between η_{sp} and concentration, the scaling exponent is 1.3 (good solvent) ~ 2.0 (θ solvent) for neutral polymer in semidilute unentangled solution [27]. And Fig. 5 shows the relationship between scaling exponent and molecular weight of PI samples in semidilute unentangled solution at 20 °C. Results are also found in Fig. S5 and Table 4. Friction between blobs can also make scaling exponent higher than theory predicts. Temperature is changed to influence blob friction coefficient. However, at other temperatures, the relationship is similar, which demonstrates that friction between blobs is irrelevant, as shown in Fig. S5. Scaling exponents are 1.68, 1.96, 2.01, 2.06, 2.17, 2.29, 2.51, and 3.37 for PI-4.1 W, PI-5.6 W, PI-6.8 W, PI-9.2 W, PI-10 W, PI-12 W, PI-14 W, and PI-20 W, respectively, and corresponding molecular weights are from 40,600 g/mol (PI-4.1 W) to 197,000 g/mol (PI-20 W). Thus, scaling exponent increases with molecular weight. PI-4.1 W and PI-5.6 W at 20–45 °C have scaling exponents of 1.60–1.96, which falls in the theoretical value of 1.3–2.0. PI-6.8 W, PI-9.2 W, PI-10 W, and PI-12 W at 20–45 °C have scaling exponents of 2.01–2.29, meanwhile PI-14 W and PI-20 W at 20–45 °C exhibits extremely high scaling exponents of 2.49–3.49.

For different PI samples, scaling exponent decreases slightly as temperature increases, except the highest molecular weight PI sample, as shown in Fig. 6. When molecular weight of PI sample reaches a critical value, the associating polymer behavior appears [22], which will be discussed in our future work.

In Fig. 7, as pointed out in our previous work [10], when effective dipole-dipole interaction space (blue circle) overlaps with other chains, the dipole-dipole interaction from inter-chained segments leads to an increase of scaling exponent. Increasing molecular weight makes both the number of beads and the intensity of inter-chained dipole-dipole interaction increase. Finally, scaling exponent is increased.

Relationship between scaling exponent and molecular weight of PI samples in semidilute entangled solution

The theory predicts that, based on the relationship between η_{sp} and concentration, the scaling exponent is 3.9 (good solvent) ~ 4.67 (θ solvent) for neutral polymer in semidilute entangled solution [27]. And Fig. 8 shows the relationship between scaling exponent and molecular weight of PI samples in semidilute entangled solution at 20 °C. Results are also found in Fig. S6 and Table 5. From 40,600 g/mol (PI-4.1 W) to 197,000 g/mol (PI-20 W), their scaling exponents are 4.58, 5.03, 5.22, 5.23, 5.39, 5.66, 6.54, respectively,

Table 5 Scaling exponents of PI samples with different molecular weights at different temperatures in semidilute entangled solution

Sample	20 °C	25 °C	30 °C	35 °C	40 °C	45 °C
PI-4.1 W	4.58 ± 0.12	4.64 ± 0.14	4.58 ± 0.06	4.56 ± 0.16	4.60 ± 0.19	4.72 ± 0.19
PI-5.6 W	5.03 ± 0.17	5.06 ± 0.15	5.00 ± 0.14	4.96 ± 0.15	4.94 ± 0.16	4.92 ± 0.18
PI-9.2 W	5.22 ± 0.13	5.20 ± 0.17	5.11 ± 0.16	5.07 ± 0.14	5.02 ± 0.13	5.01 ± 0.12
PI-10 W	5.23 ± 0.06	5.20 ± 0.07	5.14 ± 0.05	5.10 ± 0.07	5.06 ± 0.05	5.03 ± 0.08
PI-12 W	5.45 ± 0.24	5.45 ± 0.21	5.44 ± 0.23	5.41 ± 0.23	5.40 ± 0.26	5.39 ± 0.29
PI-14 W	5.66 ± 0.10	5.62 ± 0.10	5.57 ± 0.09	5.53 ± 0.11	5.51 ± 0.11	5.46 ± 0.11
PI-20 W	6.54 ± 0.16	6.51 ± 0.16	6.47 ± 0.16	6.40 ± 0.16	6.34 ± 0.16	6.31 ± 0.16

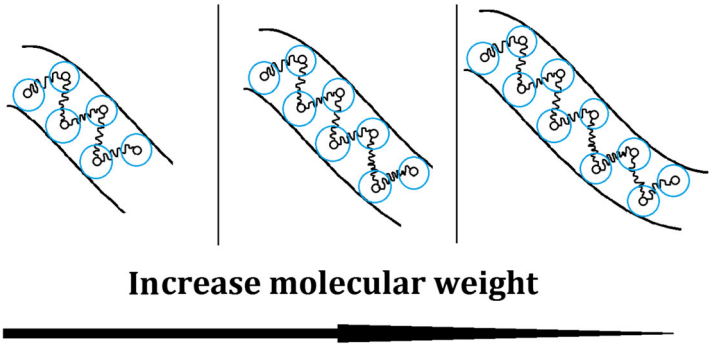

Fig. 9 Schematic of interaction between polyimide chain and tube with molecular weight of PI samples in semidilute entangled solution

which indicates that scaling exponents increase with molecular weight in semidilute entangled solution. Details for other temperatures are shown in Fig. S6. Scaling exponents for PI-4.1 W in the range of 20–45 °C are 4.56–4.72, in accordance to theoretical region of 3.9–4.67; scaling exponents for PI-5.6 W increase slightly to 4.92–5.06; scaling exponents from PI-9.2 W to PI-14 W further increase to 5.01–5.66; but scaling exponents for PI-20 W have extremely high values in the range of 6.31–6.54. If the error of experiments is considered, scaling exponents only exhibit a considerably slight decrease with raising temperature.

As mentioned above, owing to the effective dipole-dipole interaction between polyimide chain and tube, scaling exponent is higher than predicted value [10]. Figure 9 illustrates and explains related results. PI chains are confined in the tube, which is made up of surrounding PI chains. When PI solution flow rate is above a critical value, PI chains reptated and then escaped from the tube, which induced shear thinning phenomenon. However, interaction between PI chain and tube increased scaling exponent for semidilute entangled polymer solution. Increasing molecular weight made both the number of beads and the intensity of dipole-dipole interaction between polyimide chain and tube increased. Finally, scaling exponent is increased.

Relationship between overlap concentration, entanglement concentration, and molecular weight of PI samples

Figure 10 shows the relationship between overlap concentration (C^*) and molecular weight of PI samples. Different from theoretical prediction, overlap concentration C^* increased with molecular weight. For example, at 20 °C, C^*s are 1.61 wt%, 1.77 wt%, 1.81 wt%, 1.82 wt%, 1.94 wt%, 1.97 wt%, and 2.11 wt% for PI-4.1 W, PI-5.6 W, PI-6.8 W, PI-9.2 W, PI-12 W, PI-14 W, PI-20 W, respectively, corresponding to molecular weight varying from 146,000 g/mol to 407,000 g/mol. In dilute polymer solution, increasing polymer coil radius leads to a decreased C^*, and molecular weight is in proportional to polymer coil radius. As Table 1 shows, the radius of gyration increases with the molecular weight. However, current result does not obey this rule. Moreover, from Flory-Fox eq. [23]:

$$[\eta] = \phi \frac{R^3}{M} \tag{11}$$

where $\varphi = 2.5 \times 10^{23}$ mol^{-1} is universal constant for all polymer-solvent system, R is root-mean-square end-to-end

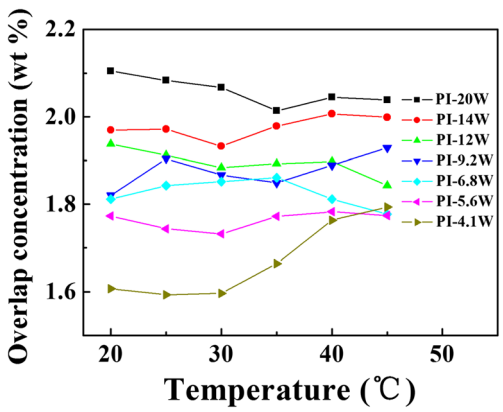

Fig. 10 Variation of the overlap concentration (C*) of PI samples with molecular weights at different temperatures

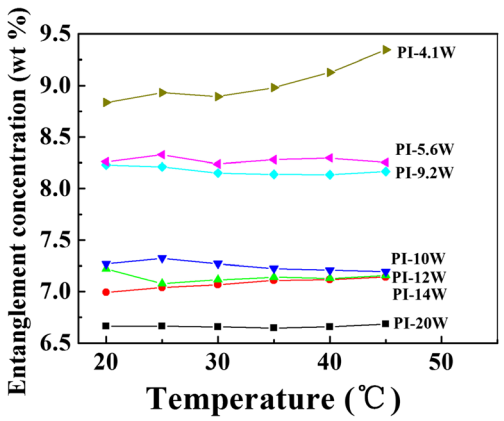

Fig. 11 Variation of the entanglement concentration (C_e) of PI samples with molecular weights at different temperatures

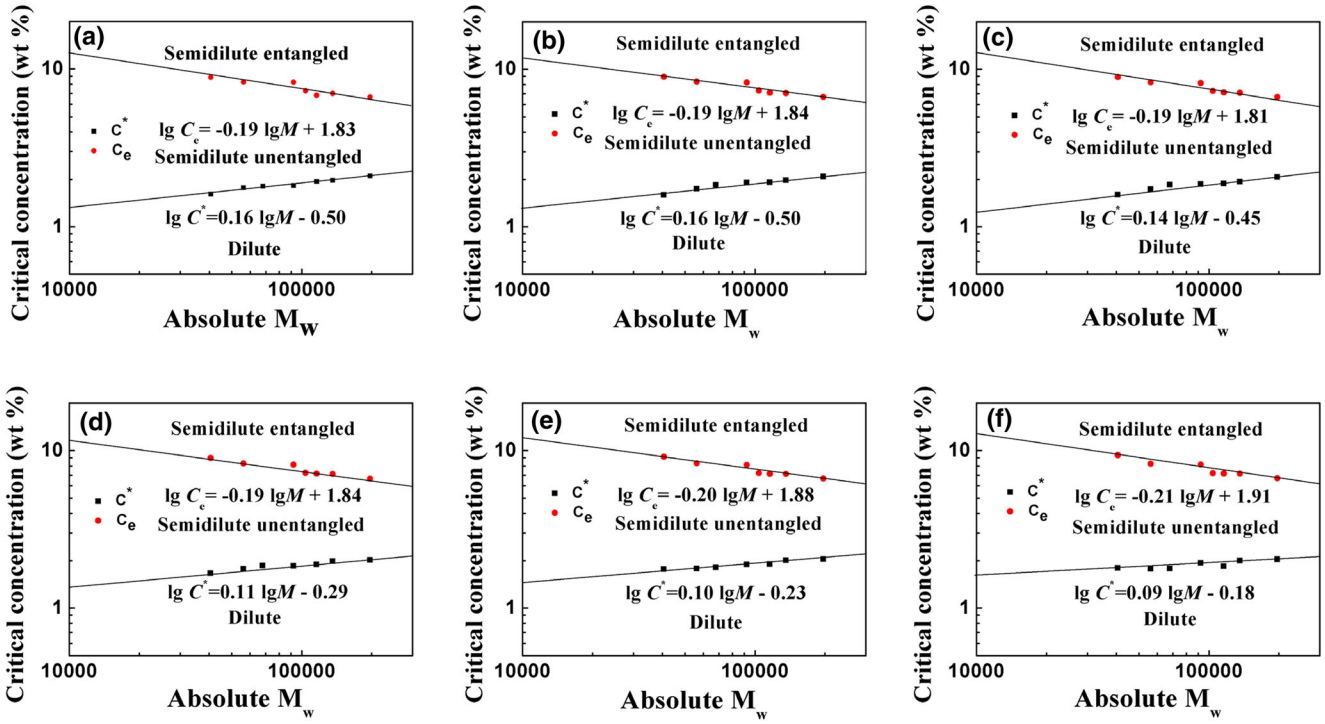

Fig. 12 Relationship between critical concentration and molecular weight of PI samples (**a**) 20 °C (**b**) 25 °C (**c**) 30 °C (**d**) 35 °C (**e**) 40 °C (**f**) 45 °C

distance, and M is molecular weight. Intrinsic viscosity is proportional to polymer coil radius, and overlap concentration is inversely proportional to $[\eta]$. Thus, analyzing $[\eta]$ can also obtain the information of overlap concentration. Two methods are applied to analyze the relationship between $[\eta]$ and molecular weight. (1) From viscometer, the relationship between $[\eta]$ and molecular weight can be analyzed directly (Fig. 1). (2) From rheometer and based on Huggins and Kraemer eq. [24, 25], the intrinsic viscosity of different molecular weight PI sample is also calculated. Results are shown in Figs. S7a, b and S8a, b. Both of them demonstrated that $[\eta]$ increases as molecular weight increases, and overlap concentration should decrease. However, overlap concentration C* calculated from intersection of specific viscosity-concentration dependence of dilute solution and semidilute unentangled solution is reversed. Thus, the reason should be explored.

Based on our previous work [10], such abnormal phenomenon on C^* can be explained. Increasing the molecular weight means the increase of the coil-coil interaction. In dilute solution, increasing the concentration makes the average distance between coils be decreased. When the distance decreases to a critical value, the interaction between coils leads to the aggregation of coils, which makes the C* larger than the neutral polymer. Finally, the C* increases with molecular weight.

Temperature also influences C^* of PI samples, and different molecular weights exhibit different cases. For PI-4.1 W, its C^* increases from 1.61 wt% to 1.79 wt% with temperatures; from PI-5.6 W to PI-9.2 W, C^* almost keeps at 1.73–1.77 wt%, 1.78–1.86 wt%, 1.82–1.92 wt% without an obvious trend with temperatures; but for PI-12 W and PI-20 W, their C^* decreases with temperatures from 1.94 wt% to 1.84 wt% for PI-12 W, and from 2.11 wt% to 2.04 wt% for PI-20 W at 20–45 °C. For PI samples with high molecular weight, raising temperature strengthens the motion of polymer chain segment, which weakens bead-bead interaction and decreases the critical distance between coils. Also, molecular weight influence becomes the major factor. Thus, this abnormal phenomenon becomes weak as temperature increases.

Figure 11 shows the relationship between entanglement concentration (C_e) and molecular weight of PI samples at different temperatures. At 20 °C, C_es are 8.84 wt%, 8.26 wt%, 8.23 wt%, 7.27 wt%, 7.22 wt%, 6.99 wt%, and 6.66 wt% for PI-4.1 W, PI-5.6 W, PI-9.2 W, PI-10 W, PI-12 W, PI-14 W, and PI-20 W, respectively. C_e decreased with molecular weight, which obeys the normal rule [26].

Further analysis on critical concentration with molecular weight

Based on above results, the relationship between critical concentration and molecular weight can be established at different temperatures (from 20 °C to 45 °C) in Fig. 12. Definitely, two linear equations are available at each temperature. For example, at 20 °C, $\lg C^* = 0.16\lg M\text{-}0.50$, $\lg C_e = -0.19\lg M + 1.83$; at 45 °C, $\lg C^* = 0.09\lg M\text{-}0.18$, $\lg C_e = -0.21\lg M + 1.91$.

It can be seen that polymer solution is divided into three regions: dilute, semidilute unentangled, and semidilute entangled solutions. If molecular weight and concentration

of one 6FDA-TFDB PI sample are known, from Fig. 12, its concentration region can be evaluated.

Moreover, C/C* ratio is an important information to judge the quality of fiber, as reported in literature [13]. For PMMA with various molecular weights, when C/C* was 0.8, only polymer droplets without any fiber are seen. When 2.9 < C/C* < 4.0, beaded fiber morphology appeared; the strength of this fiber was weak and cannot be applied. When 6.8 < C/C* < 7.2, uniform fibers are obtained [13]. Based on current relationship between critical concentration and molecular weight, it can be applied to guide the preparation of polyimide solution for different processing.

Conclusions

Based on YFY wormlike cylinder model and SEC-multidetectors results, eight 6FDA-TFDB polyimide samples are chosen to investigate the influence of molecular weight on scaling exponents and critical concentration in solution through different models: Zimm (dilute solution), Rouse–Zimm (semidilute unentangled solution), and Doi–Edwards (semidilute entangled solution). Most of the scaling exponents are higher than theoretical values in three concentration regions, and scaling exponents increase with molecular weight. Considering the corrected bead-spring model, increasing molecular weight can increase the number of beads of PI chain, which results in the increased coil-coil interaction in dilute solution, increased inter-chained dipole-dipole interaction in semidilute unentangled solution, increased intensity of dipole-dipole interaction between polyimide chain and tube in semidilute entangled solution, and increased scaling exponents at above three concentration regions. Finally, the relationship between critical concentration and molecular weight is also obtained at different temperatures, and two linear equations are available at each temperature. These results would be helpful to guide the preparation of polyimide solution for different processing.

Acknowledgements We are grateful to the financial supports from National Basic Research Program of China (2014CB643604) and National Natural Science Foundation of China (51173178).

References

1. Ding M (2007) Isomeric polyimides. Prog Polym Sci 32(6):623–628
2. Takuma A, Hiroyoshi K (2012) Ultrafine electrospun nanofiber created from cross-linked polyimide solution. Polymer 53(11): 2217–2222
3. Zhang C, Zhang Q, Xue Y, Li G, Liu F, Qiu X, Ji X, Gao L (2014) Effect of draw ratio on the morphologies and properties of BPDA/PMDA/ODA polyimide fibers. Chem Res Chin Univ 30(1):163–167
4. Qu X, Ji M, Fan L, Yang S (2011) Thermoset polyimide matrix resins with improved toughness and high T-g for high temperature carbon fiber composites. High Perf Polymer 23(4):281–289
5. Li B, Pang Y, Fang C, Gao J, Wang X, Zhang C, Liu X (2014) Influence of hydrogen-bonding interaction introduced by filled oligomer on bulk properties of blended polyimide films. J Appl Polym Sci 131(13):40498
6. Wang L, Hu A, Fan L, Yang S (2013) Approach to produce rigid closed-cell polyimide foams. High Perf Polymer 25(8):956–965
7. Dong J, Yin C, Zhao X, Li Y, Zhang Q (2013) High strength polyimide fibers with functionalized grapheme. Polymer 54(23):6415–6424
8. Wang H, Wang T, Yang S, Fan L (2013) Preparation of thermal stable porous polyimide membranes by phase inversion process for lithium-ion battery. Polymer 54(23):6339–6348
9. Matsuura T, Hasuda Y, Nishi S, Yamada N (1991) Polyimide derived from 2,2′-bis(trifluoromethyl)-4,4′-diaminobiphenyl. 1. Synthesis and characterization of polyimides prepared with 2,2′-bis(3,4-dicarboxyphenyl)hexafluoropropane dianhydride or pyromellitic dianhydride. Macromolecules 24(18):5001–5005
10. Zhang E, Dai X, Dong Z, Qiu X, Ji X (2016) Critical concentration and scaling exponents of one soluble polyimide from dilute to semidilute entangled solutions. Polymer 84:275–285
11. Liu G, Qiu X, Bo S, Ji X (2012) Chain conformation and local rigidity of soluble polyimide(II): isomerized polyimides in THF. Chem Res Chin Univ 28(2):329–333
12. Liu G, Qiu X, Siddiq M, Bo S, Ji X (2013) Temperature dependence of chain conformation and local rigidity of isomerized polyimides in dimethyl formamide. Chem Res Chin Univ 29(5):1022–1028
13. Gupta P, Elkins C, Long TE, Wilkes GL (2005) Electrospinning of linear homopolymers of poly(methyl methacrylate): exploring relationships between fiber formation, viscosity, molecular weight and concentration in a good solvent. Polymer 46(13):4799–4810
14. Fujita H (1990) Polymer solution. Elsevier, Amsterdam
15. Kratky O, Porod G (1949) Rontgenuntersuchung geloster fadenmolekule. J Roy Neth Chem Soc 68(12):1106–1122
16. Yamakawa H, Fujii M (1973) Translational friction coefficient of wormlike chains. Macromolecules 6(3):407–415
17. Bohdanecky M, Kovar J (1982) Viscosity of polymer solutions. Polymer Science Library 2, Elsevier Scientific Publishing Company, Amsterdam
18. Bohdanecky M (1983) New method for estimating the parameters of the wormlike chain model from the intrinsic viscosity of stiff-chain polymers. Macromolecules 16(9):1483–1492
19. Xu Z, Hadjichristidis N, Fetters L, Mays J (1995) Strcture/chain-flexibility relationships of polymers. Physical properties of polymers. Advance in Polymer Science, vol 120. Springer, Berlin
20. Allen FH, Kennard O, Watson DG (1987) Tables of bond lengths determined by X-ray and neutron-diffraction. 1. Bond lengths in organic-compounds. J Chem Soc Perkin Trans 2:S1–S19
21. Benoit H, Doty P (1953) Light scattering from non-gaussian chains. J Phys Chem 57(9):958–963
22. Semenov AN, Rubinstein M (1998) Dynamic of entangled solutions of associating polymers. Macromolecules 31(4):1373–1385
23. Flory PJ (1953) Principles of polymer chemistry. Cornell University Press, Ithaca
24. Huggins ML (1942) The viscosity of dilute solutions of long-chain molecules. IV Dependence on concentration J Am Chem Soc 64: 2716–2718
25. Kraemer EO (1938) Molecular weights of celluloses. Ind Eng Chem 30:1200–1203
26. Graessley WW (1980) Polymer-chain dimensions and the dependence of viscoelastic properties on concentration, molecular-weight and solvent power. Polymer 21(3):258–262
27. Rubinstein M, Colby RH (2003) Polymer physics. Oxford University Press, New York